Inorganic Chemistry

Article

pubs.acs.org/IC

Organometallic Oligomers Based on Bis(arylacetylide)bis(P-chirogenic phosphine)platinum(II) Complexes: Synthesis and Photonic Properties

Antony Lapprand,[†] Naïma Khiri,[‡] Daniel Fortin,[†] Sylvain Jugé,*[,‡] and Pierre D. Harvey*[,†,‡]

[†]Département de Chimie, Université de Sherbrooke, 2500 Boul. Université, Sherbrooke, Québec, Canada J1K 2R1

[‡]Institut de Chimie Moléculaire de l'Université de Bourgogne (ICMUB, StereochIM), Université de Bourgogne, Dijon, France

Supporting Information

ABSTRACT: A series of P-chirogenic oligomers of the type $(-C\equiv C-\mathbf{aryl}-C\equiv C-PtL_2-)_n$ [L = (*R*)- and (*S*)-P(Ph)(*i*Pr)($C_{17}H_{35}$); **aryl** = 1,4-benzene, 2,1,3-benzothiadiazole] along the corresponding achiral analogues (L = PBu_3) and model complexes $PhC\equiv CPtL_2C\equiv CPh$ were prepared from the ephedrine strategy and were fully characterized [^1H, ^{31}P NMR; IR; small-angle X-ray scattering (SAXS); gel permeation chromatography (GPC); thermal gravimetric analysis (TGA); circular dichroism, UV−vis, and luminescence spectroscopy; photophysics, and degree of anisotropy measurements]. From the CD measurements, the chiral environment of the phosphine ligands is modestly felt by the aryl moieties. Concurrently, the TGA shows that the P($C_{17}H_{35}$)(Ph)(*i*-Pr)-containing materials are more stable than those containing the shorter chain ligand PBu_3, and exhibits red-shifted absorption and emission bands compared to those including the PBu_3 ligands. The presence of the long chain on the phosphorus atoms does not greatly alter the photophysical parameters, notably the emission lifetimes, and fast triplet energy transfer terminal* → central unit has been deduced from the absence of luminescence arising from the terminal units.

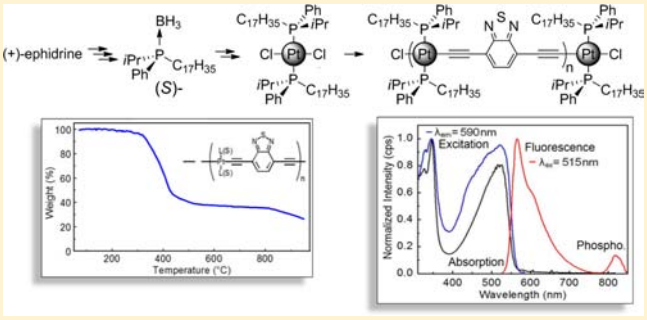

INTRODUCTION

Research on chiral polymers and macromolecules for electronic and optical properties has been the subject of intense research over the past several decades.[1] For organic polymers, research on photonic properties and applications, including polarized light sensitive photovoltaic cells,[2] polarized reflection devices,[3] polarized electroluminescence, and light emitting diodes,[4] has also been performed. The area of coordination and organometallic polymers, the design of P-containing 1-D chiral materials, is still in its infancy. To the best of our knowledge, just several chiral organometallic polymers have been reported so far. These can be separated into two categories; those whose chirality is transported by the skeleton chain,[5] notably among others, using binapthyl, and those that are P-chirogenic.[6]

Recently, our group reported a series of conjugated organometallic polymers bearing the *trans*-bis(ethynyl)bis(phosphine) unit,[7] and applications in the design of photonic devices such as photovoltaic cells[8] and light emitting diodes[9] have been made. Moreover, the rapid electronic communication across the polymeric chains, investigated by means of energy (ns) and electron transfers (fs time scale), has also been demonstrated by us.[10] To the best of our knowledge, no P-chirogenic conjugated organometallic polymer has been designed so far. One of us reported a series of articles demonstrating how to apply the ephedrine technology[11] to build P-chirogenic ligands. These chiral phosphines expectedly found applications in not only enantioselective homogeneous catalysis[12] but also cluster chemistry.[13] We now wish to report the synthesis of both enantiomers of the P-chirogenic heptadecylphenyl-*i*-propylphosphine **6** along with the organometallic conjugated polymers $(-C\equiv C-\mathbf{aryl}-C\equiv C-Pt(P(Ph)(i\text{-}Pr)(C_{17}H_{35}))_2-)_n$ (**aryl** = 1,4-benzene, 2,1,3-benzothiadiazole ((*S*)- only); Chart 1). The use of a long alkyl chain aims at verifying whether the chiral environment can be transmitted onto the π-systems of the aromatics, hence potentially altering their photonic properties.

Chart 1

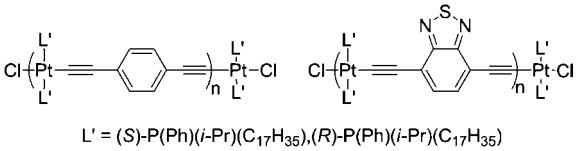

L' = (*S*)-P(Ph)(*i*-Pr)($C_{17}H_{35}$),(*R*)-P(Ph)(*i*-Pr)($C_{17}H_{35}$)

EXPERIMENTAL SECTION

Materials and General Procedure. All reactions were carried out under Ar(g) atmosphere in dried glassware with magnetic stirring.

Received: August 27, 2012
Published: February 19, 2013

 © 2013 American Chemical Society dx.doi.org/10.1021/ic301829x | *Inorg. Chem.* 2013, 52, 2361−2371

Solvents were dried prior to use. Tetrahydrofuran (THF) and toluene were distilled from sodium/benzophenone and stored under Ar(g). Dichloromethane (CH_2Cl_2) was distilled from CaH_2. Hexane and propan-2-ol for HPLC were of chromatographic grade and used without further purification. Isopropyllithium (0.7 M in pentane), methyllithium (1.6 M in Et_2O), *n*-butyllithium (2.5 M in hexane), 1-bromo-hexadecane ($C_{16}H_{33}Br$), 1,4-diazabicyclo[2.2.2]octane (DABCO), $BH_3{\cdot}SMe_2$, tributylphosphine, $K_2[PtCl_4]$, $[PdCl(\eta^3\text{-}C_3H_5)]_2$, trimethylsilylacetylene ($C_5H_{10}Si$), phenylacetylene, and copper iodide (CuI) were purchased from commercial source and used as received. (+) and (−)-Ephedrine were purchased from commercial source and dried by azeotropic shift of toluene on rotary evaporator. The toluene/HCl solution was obtained by bubbling HCl gas, and the resulting solution was titrated before use. 4,7-Bis(ethynyl)-2,1,3-benzothiadiazole was prepared according to the literature.[14] Reactions were monitored by thin-layer chromatography (TLC) using 0.25-mm precoated silica gel plates. Visualization was accomplished with UV light and/or appropriate staining reagents. Flash chromatography was performed with the indicated solvents using silica gel 60 (particle size 35−70 μm) or aluminum oxide 90 standardized. The (2*R*,4*S*,5*R*)-(+)-3,4-dimethyl-2,5-diphenyl-1,3,2-oxazaphospholidine-2-borane **2** and its enantiomer (2*S*,4*R*,5*S*)-(−)-**2** was prepared from appropriate (−)- or (+)-ephedrine, as previously described.[11] The (*Rp*)-(+)-*N*-methyl-*N*-[(1*S*,2*R*)(1-hydroxy-2-methyl-1-phenyl-2-propyl)]amino-*i*-propyl-phenylphosphine borane **3** and (*R*)-(−)- and (*S*)-(+)-methylphenyl-*i*-propylphosphine borane **4** were prepared from the (−)- or (+)-ephedrine **1**, respectively, according to the published procedure.[11a] The complexes *trans*-dichloro-bis(tris-*n*-butylphosphine)platinum(II) **8**,[15] *trans*-bis(4-ethynylbenzene)bis(tris-*n*-butylphosphine) platinum-(II) **9**,[16,17] and (+)-di-μ-chloro-bis{2[1-(dimethylamino)ethyl]phenyl-C,N}dipalladium,[18] and polymers poly(*trans*-(1,4-diethynylbenzene)-bis(tris-*n*-butylphosphine)platinum(II)) **11**[19,20] and poly[*trans*-(bis-4,7-ethynyl-2,1,3-benzothiadiazole)bis(tri-*n*-butylphosphine)platinum-(II)] **14**,[21] were prepared according to reported procedures.

(*R*)-(−)-Heptadecylphenyl-*i*-propylphosphine Borane 5. This compound is derived from (−)-ephedrine. In a two necked-flask equipped with a magnetic stirrer and an argon inlet, a solution of 2.5 g of (*R*)-(+)-methylphenyl-*i*-propylphosphine borane **4** (14.0 mmol) in THF (10 mL) is added. The mixture is cooled to 0 °C, and 11.2 mL (2.5 M in hexane, 28.1 mmol) of *n*-butyllithium is slowly added with a syringe while stirring. After the formation of a white precipitate, the mixture is stirred for 1 h at 0 °C. 1-Bromo-hexadecane (4.43 g, 14.5 mmol) is dissolved with a minimum of dry THF (5 mL) before use and added slowly. The resulting mixture was progressively warmed to room temperature and stirred for 2 h. After hydrolysis, the aqueous layer is extracted twice with dichloromethane. The organic layers were dried over anhydrous $MgSO_4$, and the solvent was removed. The residue was purified by column chromatography on silica gel using a mixture of petroleum ether/CH_2Cl_2 8:2 as eluent. Yield 56%. White solid; mp ≤ 50 °C. $[\alpha]_D^{25} = -3.2$ (c = 1.0, $CHCl_3$) for 96% ee. R_f = 0.51 (petroleum ether/CH_2Cl_2, 8:2). ^{1}H NMR (300 MHz, $CDCl_3$): δ 7.53−7.47 (m, 2H, CH_{arom}), 7.32−7.23 (m, 3H, CH_{arom}), 1.92 (m, 1H, C*H*, *i*-Pr), 1.67 (m, 2H, CH_2), 1.48 (m, 2H, CH_2), 1.03 (br s, 31H, CH_3 and $C_{17}H_{35}$), 0.93 (dd, 3H, J = 14.4, 7.3 Hz, CH_3, *i*-Pr), 0.80 (t, 3H, J = 6.2 Hz, CH_3, $C_{17}H_{35}$). ^{13}C NMR (75 MHz, $CDCl_3$): δ 132.51 (d, J = 8.0 Hz, CH_{arom}), 131.1 (d, J = 2.3 Hz, CH_{arom}), 128.6 (d, J = 9.2 Hz, CH_{arom}), 127.5 (d, J = 49.7 Hz, C_{arom}), 31.91 (s, CH_2), 31.3 (d, J = 12.7 Hz, CH_2), 29.6 (br d, J = 2.7 Hz, CH_2), 29.5 (d, J = 3.6 Hz, CH_2), 29.3 (d, J = 4.0 Hz, CH_2), 29.0 (s, CH_2), 25.1 (d, J = 35.5 Hz, CH), 23.0 (s, CH_2), 22.8 (s, CH_2), 22.7 (s, CH_2), 22.6 (s, CH_2), 16.7 (s, CH_3), 14.0 (s, CH_3). ^{31}P NMR (121 MHz, $CDCl_3$): δ +24.9 (d, J = 69.2 Hz). ESI-MS: m/z (%) = 427.4 (100) [M + Na]$^+$.

(*R*)-Heptadecylphenyl-*i*-propylphosphine 6. This compound is derived from (−)-ephedrine. In a 50 mL two-necked flask equipped with a magnetic stirrer and an argon inlet, 0.40 g of phosphine borane **5** (1.0 mmol) and 0.56 g of DABCO (5.0 mmol) were dissolved in 10 mL of toluene. The reaction mixture was heated at 50 °C for 12 h. After cooling, the crude product was rapidly transferred via a cannula into a column previously evacuated and filled with argon containing neutral alumina. The reaction solution was filtered using degassed toluene/ethyl acetate 9:1 as eluent. After removal of the solvent under vacuum/argon, the free phosphine was obtained in 98% yield. White solid. ^{1}H NMR (300 MHz, $CDCl_3$): δ 7.44−7.38 (m, 2H, CH_{arom}), 7.25−7.19 (m, 2H, CH_{arom}), 7.11 (m, 1H, CH_{arom}), 2.84 (m, 6H, C*H* and CH_2), 1.83−1.55 (m, 4H, CH_2), 1.04 (br s, 26H, CH_3 and $C_{17}H_{35}$), 0.90 (dd, 3H, J = 14.7, 7.8 Hz, CH_3, *i*-Pr), 0.78 (t, 3H, J = 7.9 Hz, CH_3, $C_{17}H_{35}$). ^{13}C NMR (75 MHz, $CDCl_3$): δ 137.6 (d, J = 16.2 Hz, C_{arom}), 133.2 (d, J = 18.8 Hz, CH_{arom}), 128.6 (br.s, CH_{arom}), 127.9 (d, J = 7.0 Hz, CH_{arom}), 31.8 (s, CH_2), 31.3 (d, J = 19.6 Hz, CH_2), 29.6 (br.s, CH_2), 29.5 (d, J = 7.5 Hz, CH_2), 29.2 (d, J = 6.0 Hz, CH_2), 27.1 (d, J = 8.3 Hz, CH), 26.1 (d, J = 14.3 Hz, CH_2), 25.1 (d, J = 12.9 Hz, CH_2), 22.6 (s, CH_2), 19.5 (s, CH_3), 19.3 (d, J = 2.3 Hz, CH_3), 14.0 (s, CH_3). ^{31}P NMR (121 MHz, $CDCl_3$): δ −7.0. The enantiomeric excess of **6** (92% ee) was determined by comparison with a racemic sample, by ^{31}P NMR in the presence of (+)-di-μ-chlorobis{2[1-(dimethylamino)ethyl]phenyl-C,N}-dipalladium.[18c] ^{31}P NMR(121 MHz, $CDCl_3$): δ + 43.0 [(*R*)-enantiomer].

(*S*)-Heptadecylphenyl-*i*-propylphosphine (*S*)-6. (Yield 98%.) This enantiomer was prepared using a similar procedure as for (*R*)-**6**, but starting from (*S*)-methylphenyl-*i*-propylphosphine borane **5**. The characterization data are identical to those for (*R*)-**6**. ^{31}P NMR (121 MHz, $CDCl_3$): δ +41.7 [(*S*)-enantiomer)].

Synthesis of the Complexes 7 [(*S*)-7 or (*R*)-7]. In a first flask, a solution of HCl 4 M (100 mL) in distilled ethanol (200 mL) was degassed with argon for 20 min, before use. In a second flask, equipped with a magnetic stirrer, an argon inlet, and a condensor, 1.0 g of phosphine **6** (2.5 mmol) and 0.40 g of $K_2[PtCl_4]$ (1.3 mmol) were introduced. The alcoholic HCl solution was then added using a cannula. The mixture was heated under reflux for 4 h, cooled at −78 °C to afford a yellow solid which was collected in the same temperature by filtration, washed with ethanol, and dried under vacuum. The resulting residue was filtered through a chromatography column on silica gel using hexane/diethyl ether, 9:1. A yellow band was obtained first, containing *trans*-{[(*i*-Pr)($C_{17}H_{35}$)(Ph)P]$_2$PtCl$_2$} (7-*trans*); eluting further with diethyl ether, an colorless band was collected, which was reduced to dryness to provide *cis*-[((*i*-Pr)($C_{17}H_{35}$)(Ph)P)$_2$PtCl$_2$] (7-*cis*). Yield 54% (ratio 7-*trans*/7-*cis*, 6:4).

***trans*-Dichlorobis[(*R*)-heptadecylphenyl-*i*-propylphosphine]platinum(II) 7-*trans*.** Yield 60%. Bright yellow solid; mp = 213-215 °C. $[\alpha]_D^{25} = -15.8$ (c = 1.0, $CHCl_3$) (derived from (−)-ephedrine). R_f = 0.80 (hexane/diethyl ether, 9:1). ^{1}H NMR (300 MHz, $CDCl_3$): δ 7.65 (m, 4H, CH_{arom}), 7.34 (m, 6H, CH_{arom}), 2.76 (m, 2H, C*H*, *i*-Pr), 2.15 (m, 4H, CH_2), 1.72 (m, 4H, CH_2), 1.39 (m, 6H, CH_2), 1.18 (br.s, 62H, CH_3 and $C_{17}H_{35}$), 0.81 (t, 6H, J = 6.0 Hz, CH_3, $C_{17}H_{35}$). ^{13}C NMR (75 MHz, $CDCl_3$): δ 133.6 (t, J = 4.0 Hz, CH_{arom}), 130.1 (s, CH_{arom}), 127.6 (t, J = 4.9 Hz, CH_{arom}), 31.9 (s, CH_2), 31.4 (t, J = 7.5 Hz, CH_2), 30.9 (s, CH), 29.7 (br.s, CH_2), 29.6 (s, CH_2), 29.5 (s, CH_2), 29.3 (s, CH_2), 29.2 (s, CH_2), 24.5 (s, CH_2), 22.7 (s, CH_2), 22.0 (t, J = 17.3 Hz, CH), 21.0 (t, J = 15.8 Hz, CH_2), 18.3 (s, CH_2), 17.4 (s, CH_3), 14.1 (s, CH_3). ^{31}P NMR (121 MHz, $CDCl_3$): δ +20.0 (s, J_{Pt-P} = 2502 Hz). ESI-MS: m/z (%) = 1068.6 (100) [M + Na]$^+$. HRMS (ESI-Q-TOF) Calcd for $C_{52}H_{94}ClP_2Pt$ [M − Cl]$^+$: 1011.6168. Found: 1011.6181. Anal. Calcd for $C_{52}H_{94}P_2PtCl_2$ (1047.25): C 59.64, H 9.05. Found: C 59.98, H 9.31.

***cis*-Dichlorobis[(*R*)-heptadecylphenyl-*i*-propylphosphine]-platinum(II) 7-*cis*.** Yield 40%. White solid; mp = 82−84 °C. $[\alpha]_D^{25}$ = −5.7 (c = 1.0, $CHCl_3$) (prepared from (*R*)-**6**). R_f = 0.10 (hexane/diethyl ether, 9:1). ^{1}H NMR (300 MHz, $CDCl_3$): δ 7.23 (t, 2H, J = 8.0 Hz, CH_{arom}), 7.05 (t, 4H, J = 7.6 Hz, CH_{arom}), 6.88 (t, 4H, J = 9 Hz, CH_{arom}), 3.28 (m, 2H, C*H*, *i*-Pr), 2.17−1.63 (m, 8H, CH_2), 1.47−1.14 (br.s, 62H, CH_3 and $C_{17}H_{35}$), 0.81 (t, 6H, J = 6.0 Hz, CH_3, $C_{17}H_{35}$), 0.48 (dd, 6H, J = 13.6, 6.2 Hz, CH_3, *i*-Pr). ^{13}C NMR (75 MHz, $CDCl_3$): δ 131.4 (t, J = 4.0 Hz, CH_{arom}), 130.4 (s, CH_{arom}), 127.8 (t, J = 4.5 Hz, CH_{arom}), 127.1 (d, J = 55.0 Hz, C_{arom}), 31.9 (s, CH_2), 31.4 (t, J = 8.3 Hz, CH_2), 29.7 (br s, CH_2), 29.6 (s, CH_2), 29.5 (s, CH_2), 29.3 (s, CH_2), 29.2 (s, CH_2), 25.2 (s, CH_2), 22.7 (s, CH_2), 19.9 (s, CH_3), 16.3 (s, CH_3), 14.1 (s, CH_3). ^{31}P NMR (121 MHz, $CDCl_3$): δ +9.7 (s, J_{Pt-P} = 3610 Hz). ESI-MS: m/z (%) = 1068.6 (100) [M + Na]$^+$. HRMS (ESI-Q-TOF) Calcd for $C_{52}H_{94}ClP_2Pt$ [M − Cl]$^+$: 1011.6168. Found: 1011.6189. Anal. Calcd for $C_{52}H_{94}P_2PtCl_2$ (1047.25): C 59.64, H 9.05. Found: C 59.62, H 9.36.

dx.doi.org/10.1021/ic301829x | *Inorg. Chem.* 2013, 52, 2361−2371

Dichlorobis[(*S*)-heptadecylphenyl-*i*-propylphosphine]-platinum(II) 7-*cis* and -*trans*. These enantiomers were prepared using a similar procedure as for (*R*)-7, but starting from (*S*)-methylphenyl-*i*-propylphosphine **6**. Their analytical data are identical to the previously described for (*R*)-7-*cis* and (*R*)-7-*trans* isomers.

Poly[*trans*-dichloro-bis(tri-*n*-butylphosphine)platinum(II)][15] 8. For comparison purposes, the characterization data are as follows: yield 68%. ^{1}H NMR (400 MHz, $CDCl_3$): δ 1.85 (m, 12H), 1.57 (m, 12H), 1.44 (m, 12H), 0.93 (t, J = 7.2 Hz, 18H). ^{31}P NMR (162 MHz, $CDCl_3$): δ +5.5 (s). m/z (EI): 670 (M^+).

Synthesis of the *trans*-Bis(ethynylphenyl)bis(phosphine)-platinum(II) Complexes. *Typical Procedure.* After three cycles of vacuum/argon in a round-bottom flask equipped with a magnetic stirrer, a dichloromethane/diisopropylamine (1:1) mixture (20 mL) was added by syringe to CuI, *trans*-$PtCl_2L_2$, and an excess of phenylacetylene. After stirring for 8 h at room temperature under argon, the solvent was removed, and the residue was purified by column chromatography on silica. The final product is yellow, which tends to crystallize. A dichloromethane−hexane mixture of 3:7 and 1:4 was used as eluent solution for the chiral complex and the achiral complex, respectively.

***trans*-Bis(1,4-ethynylbenzene)bis(tri*n*-butylphosphine)-platinum(II)[16,17] 9.** Yield 60%. ^{1}H NMR (400 MHz, $CDCl_3$): δ 7.26 (dd, J = 8.3, 1.4 Hz, 4H), 7.22−7.17 (m, 4H), 7.13−7.07 (m, 2H), 2.20−2.07 (m, 12H), 1.66−1.56 (m, 12H), 1.44 (dq, J = 14.5, 7.3 Hz, 12H), 0.92 (t, J = 7.3 Hz, 18H). ^{31}P NMR (162 MHz, $CDCl_3$): δ +4.10 (J_{P-Pt} = 2357 Hz). IR: $\nu_{(C\equiv C)}$= 2101 cm^{-1}. m/z (EI) 801.

***trans*-Bis(ethynylphenyl)bis((*S*)-heptadecylphenyl-*i*-propylphosphine)platinum(II) (*S*)-10.** Yield 85%. ^{1}H NMR (400 MHz, $CDCl_3$): δ 7.95−7.82 (m, 4H), 7.50−7.34 (m, 6H), 7.04 (tdd, J = 8.5, 5.2, 3.6 Hz, 6H), 6.89−6.71 (m, 4H), 2.97 (ddd, J = 10.1, 6.8, 3.1 Hz, 2H), 2.60−2.39 (m, 4H), 1.88−1.69 (m, 4H), 1.45−1.37 (m, 4H), 1.36−1.20 (m, 52H), 1.20−1.14 (m, 12H), 0.88 (t, J = 6.8 Hz, 6H). ^{31}P NMR (162 MHz, $CDCl_3$): δ +21.8 (J_{P-Pt} = 2521 Hz). IR: $\nu_{(C\equiv C)}$ = 2104 cm^{-1}. MS (MALDI TOF) Calcd for $PtC_{68}H_{104}P_2$: 1177.72. Found: 1177.73. Anal. Calcd for $PtC_{68}H_{104}P_2$: C 69.30, H 8.89. Found: C 69.33, H 9.19.

***trans*-Bis(ethynylphenyl)bis((*R*)-heptadecylphenyl-*i*-propylphosphine))platinum(II) (*R*)-10.** Yield 94%. ^{1}H NMR (400 MHz, $CDCl_3$): δ 7.95−7.80 (m, 4H), 7.41 (dd, J = 3.7, 1.9 Hz, 6H), 7.10−6.96 (m, 6H), 6.79 (dd, J = 8.2, 1.4 Hz, 4H), 3.01−2.92 (m, 2H), 2.60−2.40 (m, 4H), 1.84−1.67 (m, 4H), 1.45−1.37 (m, 4H), 1.36−1.20 (m, 52H), 1.20−1.14 (m, 12H), 0.88 (t, J = 6.9 Hz, 6H). ^{31}P NMR (162 MHz, $CDCl_3$): δ +22.8 (J_{P-Pt} = 2521 Hz). IR: $\nu_{(C\equiv C)}$= 2105 cm^{-1}. MS (MALDI TOF) Calcd for $PtC_{68}H_{104}P_2$: 1177.72. Found: 1177.73.

Synthesis of the Oligomers. *Typical Procedure.* A round-bottom flask equipped with a magnetic stirrer was loaded with *trans*-$PtCl_2L_2$ and an equivalent amount of 1,4-diethynylaryl and CuI in catalytic amount. After three cycles of vacuum/argon, solvent (dichloromethane/diisopropylamine (1:1) mixture) was added by syringe. After stirring for 8 h at room temperature under argon, the reaction mixture was concentrated to a minimum volume and then diluted with cold methanol until a solid precipitate was obtained, which was washed repeatedly with cold methanol and dried under vacuum.

Poly[*trans*-bis(1,4-ethynylbenzene)bis(tri*n*-butylphosphine)platinum(II)] 11. This polymer was synthesized according to literature procedure.[17] It was characterized for comparison purposes. Yield 73%. ^{1}H NMR (400 MHz, $CDCl_3$): δ 7.1 (br, 4H), 2.07 (br, 12H), 1.55 (br, 12H), 1.43 (br, 12H), 0.91 (br, 18H). ^{31}P NMR (121 MHz, $CDCl_3$): δ +8.2 (J_{P-Pt} = 2368 Hz, terminal),[20] +4.4 (J_{P-Pt} = 2356 Hz). IR: $\nu_{(C\equiv C)}$= 2099 cm^{-1}.

Poly[*trans*-bis(ethynylphenyl)bis((*R*)-heptadecylphenyl-*i*-propylphosphine)platinum(II)] (*R*)-12. Yield 78%. ^{1}H NMR (400 MHz, $CDCl_3$): δ 7.94−7.54 (br, 4H), 7.38 (m, 6H), 6.51 (br, 4H), 3.18−2.70 (m, 2H), 2.63−2.20 (m, 4H), 1.77 (br, 4H), 1.42 (br, 4H), 1.29−1.19 (m, 52H), 1.18−0.95 (m, 12H), 0.85 (t, J = 6.7 Hz, 6H). ^{31}P NMR (162 MHz, $CDCl_3$): δ +20.9 (J_{P-Pt} = 2403 Hz, terminal), +19.1 (J_{P-Pt} = 2446 Hz). IR: $\nu_{(C\equiv C)}$ = 2112 cm^{-1}. MS (MALDI TOF): >10 000. GPC (polystyrene standards): M_n = 15 700, M_w = 30 700, DPI = 1.94.

Poly[*trans*-bis(ethynylphenyl)bis[(*S*)-heptadecylphenyl-*i*-propylphosphine)platinum(II)] (*S*)-12. Yield 92%. ^{1}H NMR (400 MHz, $CDCl_3$): δ 7.83−7.52 (br, 4H), 7.37 (m, 6H), 6.51 (br, 4H), 3.14−2.78 (m, 2H), 2.64−2.25 (m, 4H), 1.82 (br, 4H), 1.41 (br, 4H), 1.25−1.19 (m, 52H), 1.07 (m, 12H), 0.85 (t, J = 6.5 Hz, 6H). ^{31}P NMR (162 MHz, $CDCl_3$): δ +20.9 (J_{P-Pt} = 2402 Hz, terminal), +19.1 (J_{P-Pt} = 2446 Hz). IR: $\nu_{(C\equiv C)}$ = 2112 cm^{-1}. MS (MALDI TOF): >10 000. Anal. Calcd for $PtC_{62}H_{98}P_2$: C 67.67, H 8.98. Found: C 67.70, H 8.79. GPC (polystyrene standards): M_n = 17 700, M_w = 30 300, DPI = 1.71.

Poly[*trans*-bis(4,7-ethynyl-2,1,3-benzothiadiazole)bis((*S*)-heptadecylphenyl-*i*-propyl phosphine)platinum(II)] (*S*)-13. Yield 78%. ^{1}H NMR (400 MHz, $CDCl_3$) δ 7.90 (s, 2H), 7.84−7.57 (m, 4H), 7.38 (s, 6H), 3.20 (d, J = 60.6 Hz, 2H), 2.86−2.37 (m, 4H), 1.82 (d, J = 45.2 Hz, 4H), 1.47−1.36 (m, 4H), 1.26−1.22 (m, 52H), 1.22−1.19 (br, 12H), 0.89−0.85 (m, 6H). ^{31}P NMR (162 MHz, $CDCl_3$): δ +24.4 (J_{P-Pt} = 2491 Hz, terminal), 21.9 (J_{P-Pt} = 2480 Hz). IR: $\nu_{(C\equiv C)}$ = 2094 cm^{-1}. Anal. Calcd for $PtC_{62}H_{96}N_2P_2S$: C 64.28, H 8.35, N 2.42, S 2.77. Found: C 64.30, H 7.98, N 2.60, S 2.58. GPC (polystyrene standards): M_n = 6050, M_w = 9500, DPI = 1.57.

Poly[*trans*-bis-(7-ethynyl-2,1,3-benzothiadiazole)bis(tri*n*-butylphosphine)platinum(II)][21] 14. Yield 78%. ^{1}H NMR (400 MHz, $CDCl_3$): δ 7.36−7.28 (m, 2H), 2.31 (br, 12H), 1.66 (br, 12H), 1.47−1.40 (br, 12H), 0.93−0.86 (br, 18H). ^{31}P NMR (162 MHz, $CDCl_3$): δ +8.1 (J_{P-Pt} = 2360 Hz, terminal), 4.29 (J_{P-Pt} = 2330 Hz). IR: $\nu_{(C\equiv C)}$ = 2090 cm^{-1}. Anal. Calcd for $PtC_{34}H_{56}N_2P_2S$: C 52.23, H 7.22, N 3.58, S 4.10. Found: C 52.20, H 7.19, N 3.30, S 3.88. GPC (polystyrene standards): M_n = 10 800, M_w = 12 900, DPI = 1.20.

Emission Quantum Yields. The quantum yields measurements[22] were performed in 2-MeTHF at 298 K. Three different measurements (i.e., different solutions) were prepared for each photophysical datum (quantum yields and lifetimes). The solutions for the samples and the reference were prepared under inert atmosphere in a glovebox. Solutions prepared for both the reference and the samples were adjusted to obtain an absorbance around 0.06 where three different solutions for each measurement were used. Each absorbance value was measured six times for better accuracy in the measurements of the quantum yields and was adjusted to be the same as much as possible for the standard and the sample for a measurement. The reference used for quantum yield was 9,10-diphenylanthracene[22b] (Φ_{298K} (2-MeTHF) = 1.0), anthracene[22c] (Φ_{298K} (MeOH) = 0.20), and H_2TPP[22d] (TPP = tetraphenylporphyrin; Φ_{298K} = 0.033).

Instruments. The NMR spectra (^{1}H, ^{13}C, and ^{31}P) were recorded on a Bruker 500 AVANCE DRX, 300 AVANCE, or 600 AVANCE II MHz spectrometer at ambient temperature or in $CDCl_3$ on a Bruker AVANCE 400 MHz FT-NMR spectrometer using tetramethylsilane as an internal standard for ^{1}H and ^{13}C nuclei or 85% H_3PO_4 as an external standard for ^{31}P nucleus at the Université de Bourgogne. All NMR spectra at the Université de Sherbrooke were acquired on a Bruker AC-300 spectrometer (^{1}H 300.15 MHz, ^{13}C 75.48 MHz, ^{31}P 121.50 MHz) or a Varian AS-400 (^{1}H 400.15 MHz, ^{31}P 162.0 MHz) using the solvent as chemical shift standard, except in ^{31}P NMR, where the chemical shifts are relative to D_3PO_4 85% in D_2O. Data are reported as s = singlet, d = doublet, t = triplet, q = quartet, m = multiplet, br s = broad singlet, integration, coupling constant(s) in Hz. Melting points were measured on a Kofler bench melting point apparatus and are uncorrected. Optical rotation values were determined at 25 °C on Perkin-Elmer 341 polarimeter, using a 10 cm quartz vessel. Mass spectral analyses were performed on BRUKER Daltonics microTOF-Q apparatus or on a BRUKER AutoflexSpeed MALDI-TOF. The circular dichroism spectra were measured in dichloromethane on a JACSO J-810 spectropolarimeter. Thermogravimetric analysis (TGA) measurements were performed on thermal gravimetric analyzer (model Perkin-Elmer TGA-6) under a nitrogen flow at a heating rate of 10 °C/min. The DSC spectra were measured on a TA Q200 differential scanning calorimeter. The gel permeation chromatography (GPC) measurements were performed on the Agilent 1050 HPLC system with VWD, using THF as eluent and polystyrene standards as calibrants. UV−vis spectra were obtained on an HP-8453 diode array spectrophotometer or on a Varian Cary 300 spectrophotometer. Emission and excitation spectra were measured on a Photon Technology International (PTI) Fluorescence QuantaMaster Series QM1 spectrophotometer. The emission lifetimes were measured on a TimeMaster model TM-3/2003 apparatus from PTI. The source

dx.doi.org/10.1021/ic301829x | *Inorg. Chem.* 2013, 52, 2361−2371

was nitrogen laser with high-resolution dye laser (fwhm ~1400 ps), and the fluorescence lifetimes were obtained from deconvolution or distribution lifetimes analysis. The uncertainties were ~50−100 ps. The phosphorescence lifetimes were performed on a PTI LS-100 using a 1 μs tungsten-flash lamp (fwhm ~1 μs). The small-angle X-ray scattering, SAXS, patterns were collected with a Bruker AXS Nanostar system equipped with a Microfocus copper anode at 45 kV/0.65 mA, MONTAL OPTICS, and a VANTEC 2000 2D detector at 67.75 mm distance from the samples calibrated with a Silver Behenate standard. The solutions were prepared saturated in distilled THF, and placed in quartz cells for measurements. The blanks were measured first and subtracted to the measured data. The diffracted intensities were then integrated from 0.15 to 5.00° 2θ and treated with Primus GNOM 3.0 program from ATSAS 2.3 software, to determine the particle sizes by pair distance distribution.[23] The collection exposure times were 2000 s/sample.

RESULTS AND DISCUSSION

Ligand Synthesis. The stereoselective synthesis of the (*R*)- and the (*S*)-monophosphine ligands **6** (as (*R*)-(−)-**6** and (*S*)-(+)-**6**; Scheme 1) was performed in several steps using the

Scheme 1. (+)-Version Leads to the Corresponding (*S*)-Derivatives

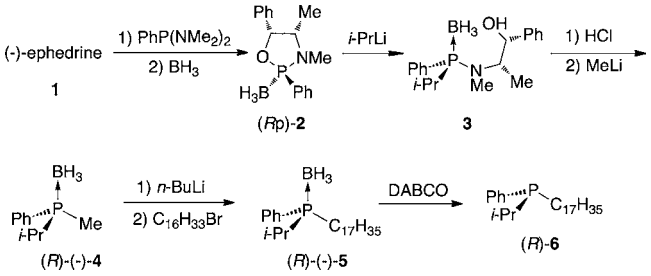

ephedrine strategy from (+)- and (−)-ephedrine where compounds **1**−**4** were already known.[11] (*R*)-(−)- and (*S*)-(+)-Methylphenyl-*i*-propylphosphine borane **4** reacts with *n*-BuLi to form the salt $LiCH_2P(BH_3)(Ph)(i\text{-}Pr)$, which reacts with $C_{16}H_{33}Br$ to generate **5** in 56% yield. Deprotection with DABCO gives the desired ligands **6** in excellent yields (98%) with an ee of 92% for (*R*)-**6**.

Synthesis and Characterization of the Model Complexes and Oligomers. The model complexes were prepared from the ligands **6**, again as the (*R*)- and (*S*)-derivatives (Scheme 2). First the platinum(II) complex **7** can be prepared from a

Scheme 2. Synthesis of the Model Complexes

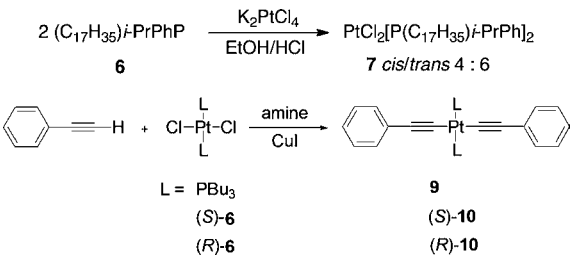

direct reaction with K_2PtCl_4. In this case, both *cis*- (40%) and *trans*- (60%) isomers were observed, isolated, and characterized. Only the *trans*-isomer was used subsequently for the preparation of the model complexes and oligomers (Schemes 2 and 3, respectively). For sake of simplicity, the nomenclature of the oligomers **10** (or **12**) prepared from the phosphine (*S*)- or (*R*)-**6**,

Scheme 3. Synthesis of the Oligomers

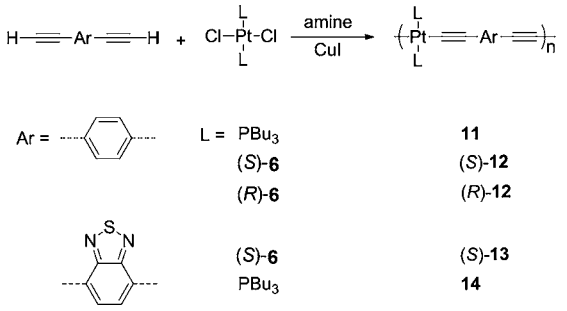

are called (*S*)-**10** or (*R*)-**10** (or (*S*)-**12** or (*R*)-**12**), respectively, independently of the absolute configuration of the phosphorus atoms.

The materials were characterized by ^1H and ^{31}P NMR, IR, and TGA, and additionally by GPC and SAXS for the oligomers. The presence of an IR signal in the 2090−2112 cm^{-1} range attests to the presence of a coordinated C≡C−Pt unit. The ^{31}P NMR resonances appear as a singlet flanked with two satellites due to the presence of ^{195}Pt (33% natural abundance). The coupling constants between the ^{31}P and ^{195}Pt nuclei are on the order of ~2350 (for the P(*n*-Bu)$_3$ ligands) and ~2450−2550 Hz (for the $P[(C_{17}H_{35})(Ph)(i\text{-}Pr)]_3$ ligands) attesting to the presence of the *trans*-geometry (details are placed in Table 1). The observation of the terminal units, $ClPtL_2$- (L = phosphine) was readily made with a distinct chemical shift and coupling constants (these are placed in the Experimental Section). The relative proportion of terminal versus central units suggests that the materials are indeed the desired oligomers. This was confirmed by GPC (Table 2) where the degree of polymerization varies between 5 and 16 units. Noteworthy, GPC measures the hydrodynamic volumes, and consequently the number of units may be somewhat overestimated. In parallel, SAXS measurements were performed, and the results indicate that the average molecular dimension for (*R*)-**12**, (*S*)-**12**, and **14** are ~4, 10, and 18 nm, respectively, while that for (*S*)-**13** is too small to be measured. On the basis of molecular modeling, 4 units of $Pt(P(C_{17}H_{35})(Ph)(i\text{-}Pr))_2\text{-}C{\equiv}CC_6H_4C{\equiv}CH$ is ~4.0 nm. This means that the materials are ~4, 10, and 18 units long for (*R*)-**12**, (*S*)-**12**, and **14**, respectively.

The accuracy of this method increases as the particle size increases, but all in all, these rigid rod oligomers are best described as polydispersed materials ranging from 4 to 18 units. This conclusion is totally consistent with the clear observation of terminal $-PtL_2Cl$ units (L = phosphine) by ^{31}P NMR. No attempt was made to increase the oligomer length. This allowed the relative amount of terminal units/central units to remain large in order to address the triplet excited state energy transfer phenomenon terminal*→central units (below). Furthermore, the shorter size of oligomers conveniently allows an easier analysis of the molecular dynamics from the measurements of the degree of anisotropy (also below).

The thermal properties of the materials were determined by thermogravimetric analysis (TGA; Figure 1). The weight loss starts being obvious (<5%) at 300 (**9**), 160 ((*R*)- and (*S*)-**10**), 350 (**11**), 370 ((*R*)- and (*S*)-**12**), 320 ((*S*)-**13**), and 150 (**14**) °C. The first derivatives of the TGA traces exhibit maxima (inflection points) and confirm the same trend (the data are placed in Table 1, see graphs in the Supporting Information (SI), Figure S1). The key feature is that there is a gain in thermal stability upon using ligand **6** over PBu_3. One may suspect that the electron-donating

dx.doi.org/10.1021/ic301829x | Inorg. Chem. 2013, 52, 2361−2371

Table 1. Comparison of the $^{31}P-^{195}Pt$ Coupling Constants, C≡C Stretching Frequencies, and Maxima of the First Derivative of the TGA Graphs

Compound or polymer	Structure (terminal unit not indicated)	J_{Pt-P} (Hz)	ν(C≡C) (cm^{-1})	T_{TGA} (°C)[a]
9	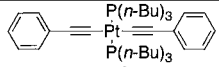	2357	2101	373
(*R*)-**10**	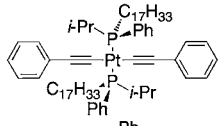	2521	2105	418
(*S*)-**10**	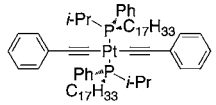	2521	2104	432
11	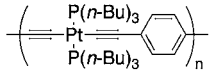	2368	2099	415
(*R*)-**12**	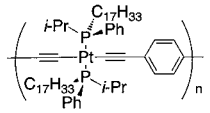	2446	2112	434
(*S*)-**12**	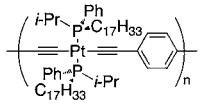	2446	2112	455
(*S*)-**13**	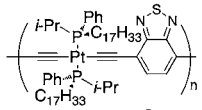	2480	2094	408
14	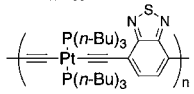	2330	2090	215

[a]Peak maxima of the first derivative of the TGA traces.

Table 2. GPC Data in THF and SAXS Results in 2-MeTHF at 298 K

polymer	M_n	M_w	PD	DP	SAXS (nm)
(*R*)-**12**	15 700	30 700	1.94	14.2	~4
(*S*)-**12**	17 700	30 300	1.71	16.1	~10
(*S*)-**13**	6050	9500	1.57	5.2	*a*
14	10 800	12 900	1.20	13.8	~18

[a]Too small to be measured.

inductive effect from the alkyl chain being stronger than that for the phenyl group makes the PBu_3 ligand a stronger base than (*R*)- and (*S*)-**6** (i.e., 3 vs 2 alkyl chains) rendering the Pt(II) center of complexes (*R*)-**10**, (*S*)-**10**, (*R*)-**12**, (*S*)-**12**, and (*S*)-**13** less electron-rich. Consequently, the more electron deficient Pt metal would attract more efficiently the C≡CR anionic ligands. With this in mind, the resulting Pt−C bond should be somewhat stronger with the (*R*)- and (*S*)-**6** ligands than PBu_3. This explanation assumes that the weak segment of the polymer is the Pt center, and yet, it is the only portion that changes.

Absorption and Circular Dichroism Spectroscopy. The absorption spectra for (*R*)-**10**, (*R*)-**12**, **13**, and **14** are presented in Figures 2 and 3 (traces in black) as representative examples (the others are placed in the SI, Figures S2 and S3), and the data are summarized in Table 3.

The nature of the electronic transitions for the materials containing $ArC{\equiv}C{-}PtL_2{-}C{\equiv}CAr$ (L = phosphine) has previously been established both experimentally and by density functional theory (DFT) and time-dependent density functional theory (TDDFT) computations. These are found to be mainly intraligand $\pi\pi^*$, but the presence of the conjugated coordinated Pt atom renders these transitions prone to be mixed with metal-to-ligand charge transfer (MLCT) or with ligand-to-metal charge transfer (LMCT). Indeed, DFT and TDDFT calculations indicate that the lowest energy electronic transition are composed of these two contributions, MLCT and LMCT.[24] For materials containing the bis-4,7-ethynyl-2,1,3-benzothiadiazole unit flanked with identical aromatics on both sides, literature indicates that a charge transfer occur from the π-system of both sides, including that of the bis-4,7-ethynyl-2,1,3-benzothiadiazole residue to the central benzothiadiazole subunit.[25] There is no theoretical study for organometallic complexes containing the bis-4,7-ethynyl-2,1,3-benzothiadiazole fragment, but it is reasonable to believe that the same scenario should occur where charge transfer excited states (more accurately stated as MLCT here) are the lowest energy states in these materials.

The optical chirality responses of the complexes and oligomers were addressed using circular dichroism spectroscopy (Figure 4). First, both (*R*)-**7** and (*S*)-**7** enantiomers were tested against the achiral complex **8**. Clear positive negative and positive responses are indeed observed between 200 and 330 nm with the strongest intensity at about 220 nm, and the spectra of the two enantiomers are the mirror image of each other. The achiral complex **8** gives the expected zero baseline. Similarly, the CD spectra for (*R*)-**10** and (*S*)-**10** exhibit positive and negative responses in the 200−360 nm window as well, where the absorption bands are located, but the signals are attenuated with respect to those for (*R*)-**7** and (*S*)-**7** for similar concentrations. Nonetheless, the chiral environments around the aromatic fragment, here benzene, are felt by the π-system. The CD spectra for (*R*)-**12** and (*S*)-**12** are

dx.doi.org/10.1021/ic301829x | Inorg. Chem. 2013, 52, 2361−2371

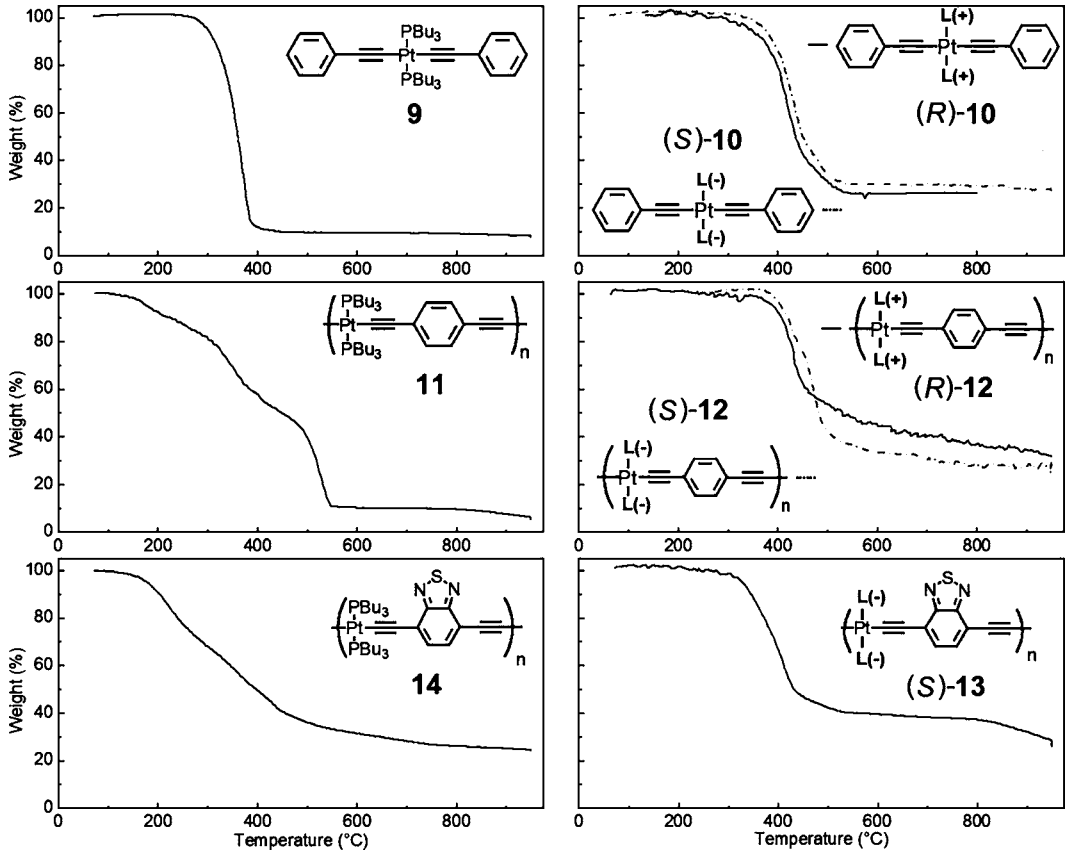

Figure 1. TGA traces of **9**–**14** (10 °C/min; N_2, 50 mL/min).

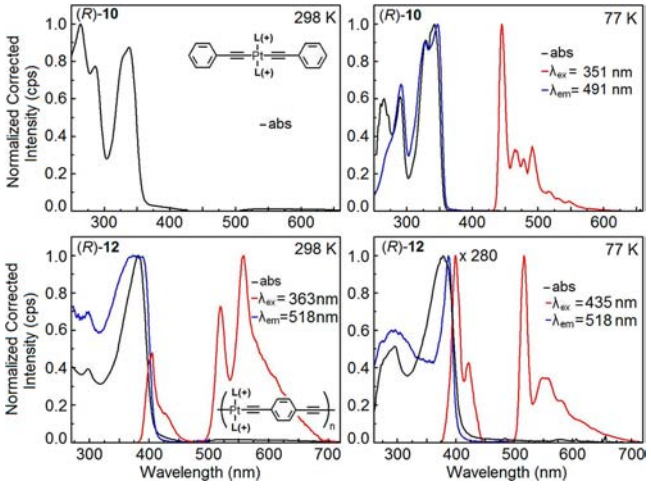

Figure 2. Absorption (black), excitation (blue), and emission (red) spectra of (*R*)-**10** (top) and (*R*)-**12** (bottom).

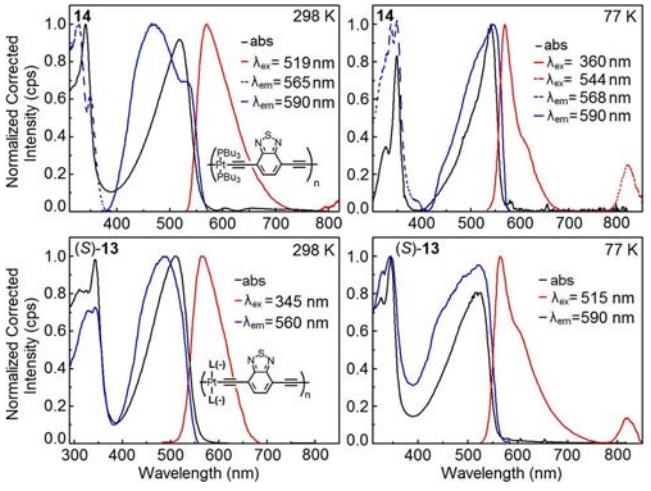

Figure 3. Absorption (black), excitation (blue), and emission (red) spectra of **14** (top) and (*S*)-**13** (bottom). The signals at ~820 nm are due to phosphorescence.

found to be even more attenuated. In one case, the signal between 280 and 420 nm, where the absorption takes place, is lost in the noisy baseline. This situation is more apparent where only a strong negative response is detected at 225 nm for polymer (*S*)-**13** (similar to that of oligomer (*S*)-**7**), and no other signal is detected above 280 nm (absorption bands are observed all the way to 550 nm), where the CD signal is compared with that for the achiral oligomer **14**. In order to address why the ligand chirality environment is not fully transmitted from the metallic unit to the aromatic, computer modeling is employed (PCModel, v. 7.0, Serena Software).

The first comparison concerns (*R*)-**7**, (*S*)-**7** vs (*R*)-**10**, (*S*)-**10**. A previous X-ray study for two geometric isomers *trans*-(2,4,6-$Me_3C_6H_2C{\equiv}C)_2(Bu_3P)_2Pt(II)$ and *trans*-(2,4,5-$Me_3C_6H_2C{\equiv}C)_2(Bu_3P)_2Pt(II)$ (Chart 2) shows that the angles formed by the average P_2PtC_2 plane with that of the aromatic one are 83.0° and 29.8°, respectively.[24h] Obviously, this phenomenon comes from a packing effect (more than intramolecular steric effect) and indicates that the rotation about the C≡C—Pt bond is possible and presumably facile. Figure 5 shows the side view and the view along the oligomer chain of oligomer (*R*)-**12** constructed with

dx.doi.org/10.1021/ic301829x | *Inorg. Chem.* 2013, 52, 2361–2371

Table 3. Absorption Data of the Materials in 2-MeTHF at 298 K

compd	λ_{max} /nm (ε /L mol^{-1} cm^{-1})
9	264 (28 200), 282 (25 300), 316 (21 500), 338 (18 800)
(*R*)-**10**	264 (28 000), 286 (21 600), 330 (25 600), 337 (26 800)
(*S*)-**10**	264 (30 500), 286 (23 800), 330 (26 500), 337 (27 800)
11	272 (3190), 301 (3800), 363 (8800)
(*R*)-**12**	268 (12 900), 298 (12 400), 362 (22 400), 386 (28 600)
(*S*)-**12**	271 (13 300), 302 (12 200), 362 (22 700), 386 (28 400)
(*S*)-**13**	315 (8000), 322 (8000), 329 (8000), 346 (10 000), 486 (9400), 515 (11 200)
14	261 (13 400), 320 (11 200), 329 (12 300), 340 (16 600), 519 (15 700)

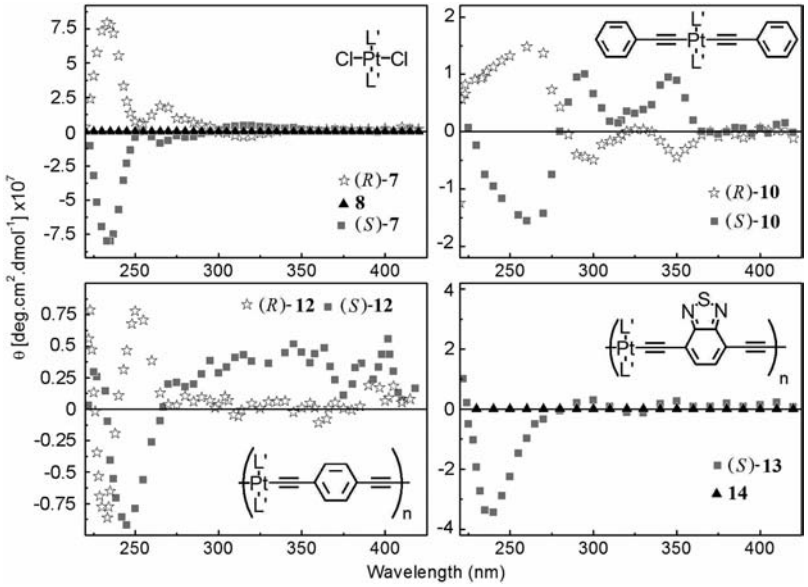

Figure 4. CD spectra of (*R*)-**7**, (*S*)-**7**, **8**, (*R*)-**10**, (*S*)-**10**, (*R*)-**12**, (*S*)-**12**, (*S*)-**13**, and **14** (in CH_2Cl_2, 298 K).

Chart 2. X-ray Angles Formed by the Average P_2PtC_2 Plane and That of the Aromatic One[24h]

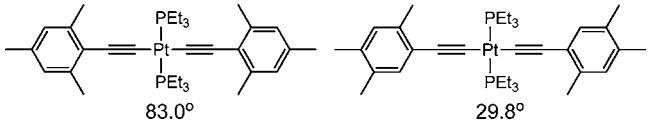

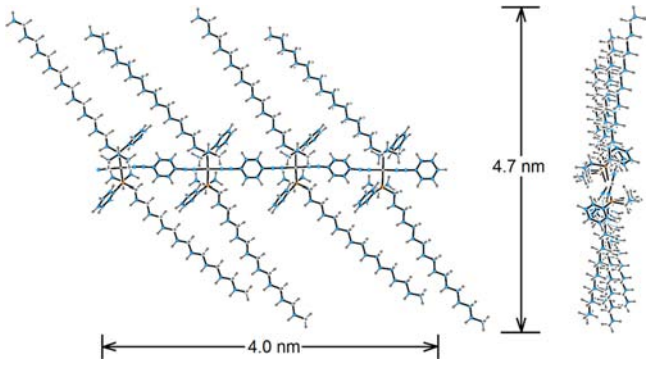

Figure 5. Side view and the view along the oligomer chain of oligomer (*R*)-**12** after energy minimization originally constructed with the building blocks placed side by side and the P_2PtC_2 planes and the $C_{17}H_{35}$ alkyl chains, perfectly parallel.

the building blocks placed side by side and the P_2PtC_2 planes and the $C_{17}H_{35}$ alkyl chains perfectly parallel. After energy minimization (*vide infra*), the $C_{17}H_{35}$ alkyl chains bend slightly toward each other and the P_2PtC_2 planes are no longer parallel, forming a screw-shaped polymer rod (Figure 5). This intrinsic structure brings a first change in local chirality from one unit to another. However, this is only a really modest alteration. Subsequently, rotating the P_2PtC_2 planes of the building blocks from one another by ~90° (attempting to minimize the proximity of the $C_{17}H_{35}$ alkyl chains) results in the collapse of these onto the oligomer backbone (Figure 6). The energy minimized structure exhibits a nonlinear (C≡C—Ar—C≡C—Pt)$_n$ central chain and different angles formed by the average P_2PtC_2 plane with that of the aromatic one.

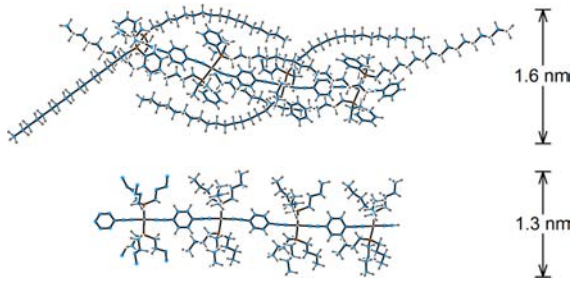

Figure 6. Top: Side view of a fragment of oligomer (*R*)-**12** after energy minimization originally constructed with the building blocks placed side by side and the P_2PtC_2 planes make an angle of ~90° with respect to each other. Bottom: Fragment of polymer **11** placed for comparison purposes.

dx.doi.org/10.1021/ic301829x | *Inorg. Chem.* 2013, 52, 2361−2371

This computer modeling along with the previous X-ray data show that the Pt−C rotation is facile and that such rotation leads to various rotamers (and combination of rotamers along the oligomer chain) making the local environment of each aromatic different. Consequently, with the environment being different, the transmission of the chiral information from the phosphine onto the π-system of the aromatic units is not homogeneous, hence resulting in a strong attenuation of the CD signals in the spectral region above >290 nm. It will be shown below that the second scenario is highly probable on the basis of anisotropy data.

Emission and Excitation Spectra. The emission and excitation spectra for (*R*)-**10**, (*R*)-**12**, **13**, and **14** (as representative examples) recorded at 298 and 77 K are presented in Figures 2 and 3 (the others are placed in the SI, Figures S2 and S3). The fluorescence and phosphorescence bands of (*R*)-**10** and (*R*)-**12** are the same as those previously reported of the achiral polymers **11** and **14** and model complexes.[21,24] The similarity in peak positions, band shapes, and activity (presence or not of fluorescence and phosphorescence) strongly suggest that the nature of the singlet (S_1) and triplet (T_1) emissive states are the same for the chiral and achiral materials. The slight variation in peak positions between the PBu_3- and $P(C_{17}H_{35})(Ph)(i\text{-}Pr)_3$-containing materials is expected due to the difference in inductive effect of the alkyl chains. The electronic bands of the latter type are all red-shifted in comparison with the former type suggesting that the $Pt[P(C_{17}H_{35})(Ph)(i\text{-}Pr)_3]_2$ unit is more electron-rich than that for $Pt(PBu_3)_2$. The fluorescence and phosphorescence quantum yields at 298 K are placed in Table 4.

Table 4. Fluorescence and Phosphorescence Quantum Yields Measured in 2-MeTHF

	298 K	
compd	Φ_F ($\times 10^{-3}$) (λ_{max}; λ_{ex}, nm)	Φ_P ($\times 10^{-3}$) (λ_{max}; λ_{ex}, nm)
11	1.34 (388; 350)	1.46 (515; 350)
(*R*)-**12**	0.26 (404; 350)	0.67 (559; 350)
(*S*)-**12**	0.25 (403; 350)	0.67 (556; 350)
(*S*)-**13**	42.4 (567; 350)	0.83 (821; 485)
14	6.82 (569; 350)	1.20 (819; 485)

Molecular Dynamic and Excited State Lifetimes. Conversely to the model complexes, the five investigated oligomers exhibit fluorescence at 298 K. This allows the measurements of the degree of anisotropy (r_0),[26] which should be important in rigid stick-shaped molecules. This method permits estimation of the change in angular displacement (β) formed by the transition moment between the moment the molecule absorbs the light and the moment it emits it. These two parameters are related by $r_0 = (^2/_5)((3\cos^2\beta - 1)/2)$.[26] For example, $\beta = 0°$, 45°, 54.7°, and 90°, and $r_0 = 0.40$, 0.10, 0.00, and −0.20, respectively. Prior to discussing the results, relevant comments are necessary. First, there are two degrees of freedom in angular displacement (β) as illustrated in Figure 7. On the basis of molecular dimensions notes in Figures 5 and 6, a rotation around the long axis (oligomer backbone) should be easier than that for the short axis. But due to the relative dimension deduced by GPC and SAXS, rotation around the short axis should also be effective, although slower.

Second, the complex $HC{\equiv}CC_6H_4C{\equiv}C{-}PtL_2{-}C{\equiv}CC_6H_4C{\equiv}CH$ (L = PBu_3; D_{2h} point group) with the *x*, *y*, and *z* axes as the long axis, the P−Pt−P axis, and the axis perpendicular to the PtP_2C_2 plane, respectively, was investigated

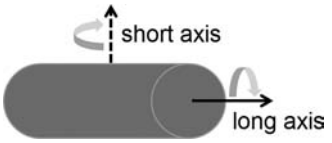

Figure 7. The two possible degrees of angular displacement in rigid rod molecules.

about 10 years ago.[27] The lowest energy excited states are $^{1,3}B_{3u}$ (^1A_g is the ground state), and the $S_0{-}S_1$ transition is allowed and polarized along the *x*-axis. This means that, for longer oligomers, the same polarization feature operates (i.e., along the long axis; Figure 7). In the light of this simple analysis, rotation around the long axis should not influence β. Conversely, rotation around the short axis should.

Oligomers **11**, (*R*)-**12**, and (*S*)-**12** exhibit fluorescence lifetimes <300 ps (Table 5). At such short time scale, the molecule does not have much time to have a significant β value (i.e., $\beta \sim 0$, $r_0 \sim 0.40$). Experimentally using $\lambda_{ex} = 370$ nm in the bulk of the lowest energy band, this expected value of ∼0.40 at the maximum intensity of the fluorescence at ∼400 nm is indeed observed (Figure 8). Conversely, the r_0 value is drastically different for the phosphorescence, which exhibits much longer lifetimes (>700 ns). A change in r_0 is obviously expected, and values approaching 0 (meaning $\beta \sim 54.7°$ (magic angle)) are expected (i.e., the rigid rods have time to tumble prior to emission).

For oligomers (*S*)-**13** and **14**, the fluorescence lifetimes are ∼4 times longer allowing enough time for reorganization of the oligomer orientations in solution. The minimum r_0 values (at maximum intensity where it is more accurate) are approximately −0.20 and approximately −0.15 for (*S*)-**13** and **14**, respectively (Figure 9). These values suggest β values of ∼90° (maximum possible) and ∼80°, respectively. This result is in line with the GPC and SAXS data (Table 2), which implies that shorter oligomers (here (*S*)-**13**) should tumble more easily (therefore changing their relative orientation) than longer ones (here **14**). However, the similarity in r_0 and β values indicates that both must have a similar dominant reorganization motion in solution. The common reorientation must be the rotation along the *x* axis with a polymer conformation resembling that shown in Figure 6.

Interestingly, despite the clear evidence of significant amount of terminal $-C{\equiv}C{-}PtL_2Cl$ (L = PBu_3) units from the ^{31}P NMR, the corresponding blue-shifted phosphorescence is not observed. The expected signal is at $\lambda_{em}(0{-}0) = 435$ nm, previously reported for $PhC{\equiv}C{-}Pt(PBu_3)_2Cl$.[20] Moreover, the phosphorescence decays appear as a single exponential in all cases, excluding the possibility of having this emission blurred by the more intense phosphorescence of the central units (i.e., $PtL_2{-}C{\equiv}CC_6H_4C{\equiv}C{-}PtL_2$). Recently, evidence of emissions arising from both the terminal and central units was provided for oligomers comprising the $-C{\equiv}C{-}PtL_2{-}C{\equiv}C-$ (L = PBu_3) or $C{\equiv}C{-}Pt_2(dppm)_2{-}C{\equiv}C$ bridge (Figure 10).[28]

In these cases, the lowering of the phosphorescence lifetimes of the end groups versus their model compounds implied the presence of triplet energy transfers terminal*→central. The rates, $k_{ET}(T_1)$, are extracted from $k_{ET}(T_1) = (1/\tau_e) - (1/\tau_e^o)$ where τ_e and τ_e^o are the emission lifetimes of the donor, here the $-C{\equiv}C{-}PtL_2Cl$ end group (as the 0−0 peak is expected at 435 nm), in the presence and the absence of the acceptor, and here the central units (as the 0−0 peak is at 443 nm, 77 K),

dx.doi.org/10.1021/ic301829x | *Inorg. Chem.* 2013, 52, 2361−2371

Table 5. Fluorescence and Phosphorescence Lifetimes in 2-MeTHF[a]

compd	298 K τ_F (ns)	298 K τ_P (ns)	77 K τ_F (ns)	77 K τ_P (μs)
9				31.7 ± 2.4 (443)
(*R*)-**10**				33.2 ± 0.2 (445)
(*S*)-**10**				34.2 ± 0.7 (445)
11	<0.10 (400)[b]	0.75 ± 0.03 (515)	0.20 ± 0.04 (440)	53.0 ± 0.4 (515)
(*R*)-**12**	0.27 ± 0.03 (400)	26.9 ± 1.5 (555)	0.31 ± 0.03 (440)	45.6 ± 2.6 (515)
(*S*)-**12**	0.16 ± 0.02 (400)	22.1 ± 1.5 (555)	0.35 ± 0.09 (440)	48.1 ± 0.1 (518)
(*S*)-**13**	1.22 ± 0.21 (560)		0.45 ± 0.05 (570)	
14	1.26 ± 0.30 (560)		0.38 ± 0.06 (570)	

[a]The values in parentheses are the emission positions where the measurements were performed. The phosphorescence lifetime at 800 nm for (*S*)-**13** and **14** could not be measured due to the low intensity of the signal in this region. [b]Reached detection limit.

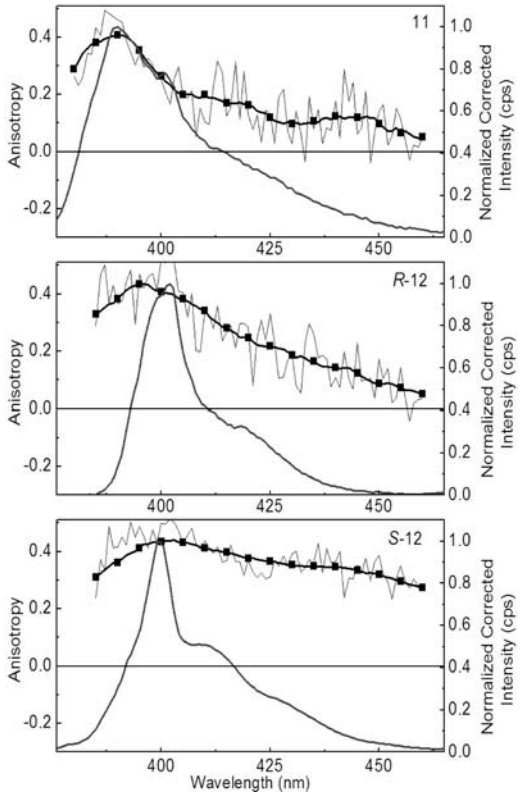

Figure 8. Measurements of the degree of anisotropy (r_0) for **11**, (*R*)-**12**, and (*S*)-**12** in 2-MeTHF at 298 K: $r_0 = ((I_\parallel/I_\perp) - 1)/((I_\parallel/I_\perp) + 2)$ with $(I_\parallel/I_\perp) = (I_{VV}I_{HH})/(I_{VH}I_{HV})$ with I_{VV} being the emission intensity measured using a vertically and vertically placed polarizers at the excitation and emission positions, and so on. H means horizontally (λ_{ex} = 370 nm).

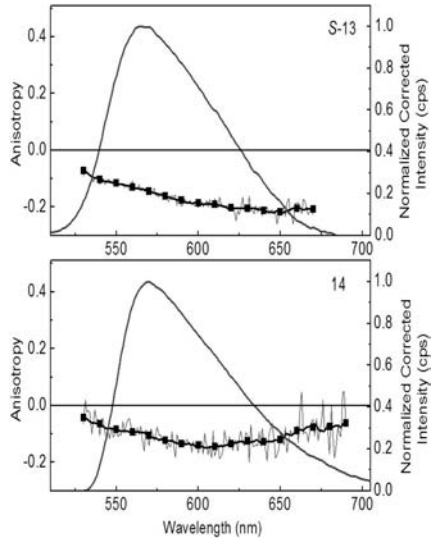

Figure 9. Measurements of the degree of anisotropy (r_0) for (*S*)-**13** and **14** in 2-MeTHF at 298 K: $r_0 = ((I_\parallel/I_\perp) - 1)/((I_\parallel/I_\perp) + 2)$ with $(I_\parallel/I_\perp) = (I_{VV}I_{HH})/(I_{VH}I_{HV})$ with I_{VV} being the emission intensity measured using a vertically and vertically placed polarizers at the excitation and emission position, and so on. H means horizontally.[26].

respectively. The $k_{ET}(T_1)$ values range from 0.1 × 10^5 to 3.3 × 10^5 s^{-1} for structurally related oligomers (Figure 10). We conclude that a fast triplet energy transfer terminal*→central takes places, presumably with rates larger than 3.3 × 10^5 s^{-1}, where evidence for the donor emission is still detectable.

CONCLUSION

The ligands (*R*)-**6** and (*S*)-**6** were prepared in several steps using the ephedrine strategy from (+)- and (−)-ephedrine in ee up to 98%, hence demonstrating its utility. From these chiral species, three oligomers containing the unit (*R*)- or (*S*)-*trans*-Pt[P-$(C_{17}H_{35})$(Ph)(*i*-Pr)$_3$]$_2$ have been prepared using the bis-1,4-ethynylbenzene and bis-4,7-ethynyl-2,1,3-benzothiadiazole as bridges. To the best of our knowledge, these new materials are the first P-chirogenic conjugated polymers (as oligomers) to be reported. They were compared to the achiral analogues containing the *trans*-Pt[P(PBu$_3$)$_3$]$_2$ fragment, and several differences were noted. First, the P($C_{17}H_{35}$)(Ph)(*i*-Pr)$_3$-containing materials are more thermally stable than that containing the shorter chain ligand PBu$_3$. Second, presumably based on inductive effect, the *trans*-Pt(P($C_{17}H_{35}$)(Ph)(*i*-Pr))$_2$-containing oligomers exhibit absorption and emission bands that are more red-shifted than those bearing the *trans*-Pt(PBu$_3$)$_2$ residue. Third, the through space transmission of the chirality environment to the π-systems of the aromatic bridges is attenuated in the oligomers, presumably because of the irregular environment from one unit to the next in the chain based on computer modeling. Fourth, the presence of the long chain on the phosphorus atoms does not greatly alter the photophysical parameters, notably the emission lifetimes. This means that the long chain must be placed away from the lumophore, which is located in the middle of the oligomer skeleton. Fifth, the oligomer nature of the materials conveniently allows demonstrating that a fast triplet energy transfer terminal*→central takes places. The comparison with rates for structurally related systems indicates that the rates must be faster than 3.3 × 10^5 s^{-1}. These observations and conclusions on the structure−property relationship are clearly useful for the future design photonic materials bearing chiral moieties.

dx.doi.org/10.1021/ic301829x | Inorg. Chem. 2013, 52, 2361−2371

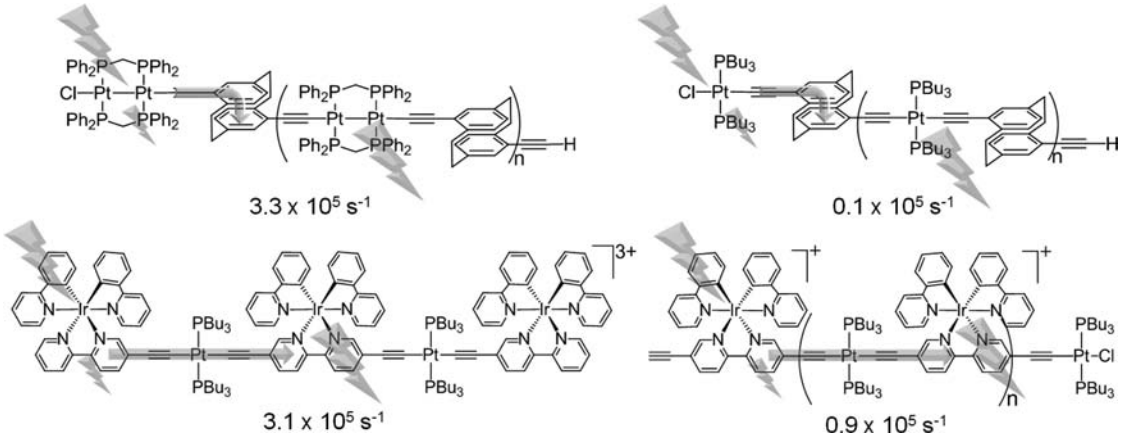

Figure 10. Structures of the known oligomers exhibiting emissions from the terminal and central units.

■ ASSOCIATED CONTENT

Supporting Information

Absorption, excitation, and emission spectra of **9**, **11**, (*S*)-**10**, and (*S*)-**12**; TGA 1st derivatives traces of **9**−**14**; table giving the peak positions in the emission and excitation spectra; table giving the CD spectroscopic data; and the NMR spectra. This material is available free of charge via the Internet at http://pubs.acs.org.

■ AUTHOR INFORMATION

Corresponding Author

*E-mail: Pierre.Harvey@USherbrooke (P.D.H.); Sylvain.Juge@u-bourgogne.fr (S.J.). Phone: 1-819-821-7092 (P.D.H.); +33 (0) 3 80 39 61 13 (S.J.).

Notes

The authors declare no competing financial interest.

■ ACKNOWLEDGMENTS

This research was supported by the Natural Sciences and Engineering Research Council of Canada (NSERC), le Fonds Québécois de la Recherche sur la Nature et les Technologies (FQRNT), the Centre d'Etudes des Matériaux Optiques et Photoniques de l'Université de Sherbrooke (CEMOPUS) and l'Agence Nationale de la Recherche (France) for the grant *MetChirPhos* and the Award of a Research chair of Excellence to P.D.H.. We thank Dr. Pierre Lavigne (Faculté de Médecine of the Université de Sherbrooke) for letting us use his circular dichroism spectrometer and Dr. J. Bayardon for helpful discussion and his help in the preparation of this manuscript.

■ REFERENCES

(1) Lin, P. *Macromol. Rapid Commun.* **2000**, *21*, 795−809.

(2) (a) Schenning, A. P. H. J.; Fransen, M.; van Duren, J. K. J.; van Hal, P. A.; Janssen, R. A. J.; Meijer, E. W. *Macromol. Rapid Commun.* **2002**, *23*, 271−275. (b) Gilot, J.; Abbel, R.; Lakhwani, G.; Meijer, E. W.; Schenning, A. P. H. J.; Meskers, S. C. J. *Adv. Mater.* **2010**, *22*, E131−E134.

(3) Lakhwani, G.; Meskers, S. C. J. *J. Phys. Chem. Lett.* **2011**, *2*, 1497−1501.

(4) (a) Oda, M.; Nothofer, H.-G.; Lieser, G.; Scherf, U.; Meskers, S. C. J.; Neher, D. *Adv. Mater.* **2000**, *12*, 362−365. (b) An, Z.; Yin, J.; Shi, N.; Jiang, H.; Chen, R.; Shi, H.; Huang, W. *J. Polym. Sci., Part A: Polym. Chem.* **2010**, *48*, 3868−3879. (c) Godbert, N.; Burn, P. L.; Gilmour, S.; Markham, J. P. J.; Samuel, I. D. W. *Appl. Phys. Lett.* **2003**, *83*, 5347−5350. (d) Dautel, O. J.; Wantz, G.; Flot, D.; Lere-Porte, J.-P.; Moreau, J. J. E.; Parmeix, J.-P.; Serein-Spirau, F.; Vignau, L. *J. Mater. Chem.* **2005**, *15*, 4446−4452. (e) Catellani, M.; Luzzati, S.; Bertini, F.; Bolognesi, A.; Lebon, F.; Longhi, G.; Abbate, S.; Famulari, A.; Valdo Meille, S. *Chem. Mater.* **2002**, *14*, 4819−4826. (f) Steiger, D.; Weder, C. *Opt. Sci. Eng.* **2007**, *111*, 451−481. (g) Endo, T.; Rikukawa, M.; Sanui, K. *Synth. Met.* **2001**, *119*, 191−192. (h) Oda, M.; Meskers, S. C. J.; Nothofer, H. G.; Scherf, U.; Neher, D. *Synth. Met.* **2000**, *111*−*112*, 575−577.

(5) Onitsuka, K.; Harada, Y.; Takahashi, S. *Synth. Met.* **2009**, *159*, 982−985. (b) Nasser, N.; Puddephatt, R. J. *Chem. Commun.* **2011**, *47*, 2808−2810. (c) Alam, Md. A.; Tsuda, A.; Sei, Y.; Yamaguchi, K.; Aida, T. *Tetrahedron* **2008**, *64*, 8264−8270.

(6) (a) Salomon, C.; Fortin, D.; Khiri, N.; Jugé, S.; Harvey, P. D. *Eur. J. Inorg. Chem.* **2011**, 2597−2609. (b) Ouchi, Y.; Morisaki, Y.; Ogoshi, T.; Chujo, Y. *Chem.—Asian J.* **2007**, *2*, 397−402.

(7) Wong, W.-Y.; Harvey, P. D. *Macromol. Rapid Commun.* **2010**, *31*, 671−713.

(8) Zhan, H.; Lamare, S.; Ng, A.; Kenny, T.; Guernon, H.; Chan, W.-K.; Djurisic, A. B.; Harvey, P. D.; Wong, W.-Y. *Macromolecules* **2011**, *44*, 5155−5167.

(9) (a) Goudreault, T.; He, Z.; Guo, Y.; Ho, C.-L.; Wang, Q.; Zhan, H.; Wong, K.-L.; Fortin, D.; Yao, B.; Xie, Z.; Kwok, W.-M.; Wong, W.-Y.; Harvey, P. D. *Macromolecules* **2010**, *43*, 7936−7949. (b) Ho, C.-L.; Chui, C.-H.; Wong, W.-Y.; Aly, S. M.; Fortin, D.; Harvey, P. D.; Yao, B.; Xie, Z.; Wang, L. *Macromol. Chem. Phys.* **2009**, *210*, 1786−1798.

(10) (a) Aly, S. M.; Ho, C.-L.; Wong, W.-Y.; Fortin, D.; Harvey, P. D. *Macromolecules* **2009**, *42*, 6902−6916. (b) Aly, S. M.; Ho, C.-L.; Wong, W.-Y.; Abd-El-Aziz, A. S.; Harvey, P. D. *Chem.—Eur. J.* **2008**, *14*, 8341−8352.

(11) (a) Chaux, F.; Frynas, S.; Laureano, H.; Salomon, C.; Morata, G.; Auclair, M.-L.; Stephan, M.; Merdès, R.; Richard, P.; Ondel-Eymin, M.-J.; Henry, J. C.; Bayardon, J.; Darcel, C.; Jugé, S. *C. R. Chim.* **2010**, *12*, 1213−1226. (b) Darcel, C.; Uziel, J.; Jugé, S. In *Phosphorus Ligands in Asymmetric Catalysis Synthesis and Applications*; Börner, A., Ed.; Wiley-VCH: New York, 2008; Vol. 3, p 1211. (c) Bauduin, C.; Moulin, D.; Kaloun, E. B.; Darcel, C.; Jugé, S. *J. Org. Chem.* **2003**, *11*, 4293−4301. (d) Kaloun, E. B.; Merdès, R.; Genêt, J. P.; Uziel, J.; Jugé, S. *J. Organomet. Chem.* **1997**, *529*, 455−463. (e) Jugé, S.; Stéphan, M.; Merdès, R.; Genêt, J. P.; Halut-Desportes, S. *J. Chem. Soc., Chem Commun* **1993**, 531−532. (f) Jugé, S.; Stéphan, M.; Laffitte, J. A.; Genêt, J. P. *Tetrahedron Let.* **1990**, *31*, 6357−6360.

(12) (a) León, T.; Parera, M.; Roglans, A.; Riera, A.; Verdaguer, X. *Angew. Chem., Int. Ed.* **2012**, *51*, 1−6. (b) Patureau, F. W.; Siegler, M. A.; Spek, A. L.; Sandee, A. J.; Jugé, S.; Aziz, S.; Berkessel, A.; Reek, J. N. H. *Eur. J. Inorg. Chem.* **2012**, 496−503. (c) Stephan, M.; Modec, B.; Mohar, B. *Tetrahedron Lett.* **2011**, *52*, 1086−89. (d) Khiri, N.; Bertrand, E.; Ondel-Eymin, M.-J.; Rousselin, Y.; Bayardon, J.; Harvey, P. D.; Jugé, S. *Organometallics* **2010**, 3622−3631. (e) Darcel, C.; Moulin, D.; Henry, J.-C.; Lagrelette, M.; Richard, P.; Harvey, P. D.; Jugé, S. *Eur. J. Org. Chem.* **2007**, *13*, 2078−2090. (f) Grabulosa, A.; Muller, G.; Ordinas, J. I.; Mezzetti, A.; Maestro, M. A.; Font-Bardia, M.; Solans, X. *Organometallics* **2005**, *24*, 4961−4973. (g) Colby, E. A.; Jamison, T. F. *J. Org. Chem.* **2003**, *68*, 156−166. (h) Maienza, F.; Spindler, F.; Thommen, M.; Pugin,

B.; Malan, C.; Mezzetti, A. *J. Org. Chem.* **2002**, *67*, 5239−5249. (i) Nettekoven, U.; Widhalm, M.; Kalchhauser, H.; Kamer, P. J. C.; Van Leeuwen, P. W. N. M.; Lutz, M.; Spek, A. L. *J. Org. Chem.* **2001**, *64*, 759−770. (j) Nettekoven, U.; Widhalm, M.; Kamer, P. C. J.; van Leeuwen, P. W. N. M.; Mereiter, K.; Lutz, M.; Spek, A. L. *Organometallics* **2000**, *19*, 2299−2309. (k) Ewalds, R.; Eggeling, E. B.; Hewat, A. C.; Kamer, P. C.J .; van Leeuwen, P. W. N. M.; Vogt, D. *Chem.—Eur. J.* **2000**, *6*, 1496−1504. (l) Nettekoven, U.; Kamer, P. J. C.; Van Leeuwen, P. W. N. M.; Wildhalm, M.; Spek, A.; Lutz, M. *J. Org. Chem.* **1999**, *64*, 3996−4004. (m) Maienza, F.; Wörle, M.; Steffanut, P.; Mezzetti, A.; Spindler, F. *Organometallics* **1999**, *18*, 1041−1049.

(13) (a) Salomon, C.; Dal Molin, S.; Fortin, D.; Mugnier, Y.; Boeré, R. T.; Jugé, S.; Harvey, P. D. *Dalton* **2010**, *39*, 10068−10075. (b) Salomon, C.; Fortin, D.; Darcel, C.; Jugé, S.; Harvey, P. D. *J. Cluster Sci.* **2009**, *20*, 267−280.

(14) DaSilveira, N. B. A.; Sant'Ana Lopes, A.; Ebeling, G.; Gonçalves, R. S.; Costa, V. E. U.; Quina, F. H; Dupont, J. *Tetrahedron* **2005**, *61*, 10975−10982.

(15) Kauffman, G. B.; Teter, L. A. *Inorg. Synth.* **1963**, *7*, 245−249.

(16) Rogers, J. E.; Cooper, T. M.; Fleitz, P. A.; Glass, D. J.; McLean, D. G. *J. Phys. Chem. A* **2002**, *106*, 10108−10115.

(17) Ramakrishna, G.; Goodson, T., III; Rogers-Haley, J. E.; Cooper, T. M.; McLean, D. G.; Urbas, A. *J. Phys. Chem. C* **2009**, *113*, 1060−1066.

(18) (a) Tani, K.; Brown, L. D.; Ahmed, J.; Ibers, J. A.; Yokota, M.; Nakamura, A.; Otsuka, S. *J. Am. Chem. Soc.* **1977**, *99*, 7876−7886. (b) Ollis, W. D.; Rey, M.; Sutherland, I. O. *J. Chem. Soc., Perkin Trans. I* **1983**, 1009−1027. (c) Dunina, V. V.; Kuz'mina, L. G.; Kazakova, M. Y.; Grishin, Y. K.; Veits, Y. A.; Kazakova, E. I. *Tetrahedron: Asymmetry* **1997**, *8*, 2537−2545.

(19) Zhao, X.; Cardolaccia, T.; Farley, R. T.; Abboud, K. A.; Schanze, K. S. *Inorg. Chem.* **2005**, *44*, 2619−2627.

(20) Cooper, T. M.; Krein, D. M.; Burke, A. R.; McLean, D. G.; Rogers, J. E.; Slagle, J. E.; Fleitz, P. A. *J. Phys. Chem. A* **2006**, *110*, 4369−4375.

(21) (a) Kohler, A.; Wilson, J. S.; Friend, R. H.; Al-Suti, M. K.; Khan, M. S.; Gerhard, A.; Bassler, H. *J. Chem. Phys.* **2002**, *116*, 9457−9463. (b) Koehler, A.; Beljonne, D. *Adv. Funct. Mater.* **2004**, *14*, 11−18.

(22) (a) Demas, J. N.; Crosby, G. A. *J. Phys. Chem.* **1971**, *75*, 991−1024. (b) Gagnon, K.; Aly, S. M.; Fortin, D.; Abd-El-Aziz, A. S.; Harvey, P. D. *J. Inorg. Organomet. Polym. Mater.* **2009**, *19*, 28−34. (c) Hu, Y.; Geissinger, P.; Woehl, J. C. *J. Lumin.* **2011**, *131*, 477−481. (d) Gros, C. P.; Brisach, F.; Meristoudi, A.; Espinosa, E.; Guilard, R.; Harvey, P. D. *Inorg. Chem.* **2007**, *46*, 125−35.

(23) Putnam, C. D.; Hammel, M.; Hura, G. L.; Tainer, J. A. *Q. Rev. Biophys.* **2007**, *40*, 191−285.

(24) (a) Masai, H.; Sonogashira, K.; Hagihara, N. *Bull. Chem. Soc. Jpn.* **1971**, *44*, 2226−2230. (b) Cooper, T. M.; Blaudeau, J.-P.; Hall, B. C.; Rogers, J. E.; McLean, D. G.; Liu, Y.; Toscano, J. P. *Chem. Phys. Lett.* **2004**, *400*, 239−244. (c) Pan, Q.-J.; Fu, H.-G.; Yu, H.-T.; Zhang, H.-X. *Inorg. Chim. Acta* **2006**, *359*, 3306−3314. (d) Minaev, B.; Jansson, E.; Lindgren, M. *J. Chem. Phys.* **2006**, *125*, 094306/1−094306/11. (e) Cooper, T. M.; Krein, D. M.; Burke, A. R.; McLean, D. G.; Rogers, J. E.; Slagle, J. E. *J. Phys. Chem. A* **2006**, *110*, 13370−13378. (f) Glusac, K.; Köse, M. E.; Jiang, H.; Schanze, K. S. *J. Phys. Chem. B* **2007**, *111*, 929−940. (g) Batista, E. R.; Martin, R. L. *J. Phys. Chem. A* **2005**, *109*, 9856−9859. (h) Gagnon, K.; Aly, S. M.; Brisach-Wittmeyer, A.; Bellows, D.; Berube, J.-F.; Caron, L.; Abd-El-Aziz, A. S.; Fortin, D.; Harvey, P. D. *Organometallics* **2008**, *27*, 2201−2214.

(25) (a) Yang, Z.-D.; Feng, J.-K.; Ren, A.-M. *J. Mol. Struct.* **2008**, *848*, 24−33. (b) Zhang, H.; Wan, X.; Xue, X.; Li, Y.; Yu, A.; Chen, Y. *Eur. J. Org. Chem.* **2010**, *9*, 1681−1687.

(26) Lakowicz, J. R. *Principles of Fluorescence Spectroscopy*, 2nd ed.; Springer: New York, 2004; Chapter 10.

(27) Emmert, L. A.; Choi, W.; Marshall, J. A.; Yang, J.; Meyer, L. A.; Brozik, J. A. *J. Phys. Chem. A* **2003**, *107*, 11340−11346.

(28) (a) Clément, S.; Goudreault, T.; Bellows, D.; Fortin, D.; Guyard, L.; Knorr, M.; Harvey, P. D. *Chem. Commun.* **2012**, *48*, 8640−8642. (b) Soliman, A. M.; Fortin, D.; Zysman-Colman, E.; Harvey, P. D. *Chem. Commun.* **2012**, *48*, 6271−6273.